High Pressure/ Low Temperature Polymorphism in 2,6-Dimethylpyridine Formic Acid Cocrystals.

Rachael Lee,[a] *Dmitry S. Yufit,*[a] *Michael R. Probert,*[b*] *Jonathan W. Steed.*[a]

[a]Durham University, South Road, Durham, DH1 3LE

[a]Newcastle University, King's Road, Newcastle-Upon-Tyne, NE1 7RU

Abstract

Five new cocrystals of 2,6-dimethylpyridine (DMP) with formic acid (FA) were crystallized by application of pressure in a diamond anvil cell and by *in situ* cryo-crystallization. Mixtures in ratios 1:1, 1:2 and 1:3 of DMP: FA have crystallized *via* both methods. Both the 1:2 and 1:3 cocrystals exhibit high pressure/low temperature polymorphism.

Introduction

The application of pressure, using equipment such as the diamond anvil cell (DAC), is a versatile method of exploring a substance's solid form landscape. The technique has grown in popularity as well as capacity in recent years.[1, 2] Conventionally, temperature variation is one of the primary means used to crystallize molecular species both from solution and from the melt. Temperature-dependent polymorphism is a commonly observed phenomenon. Pressure offers another dimension on the pressure-temperature landscape with which to probe the behavior and characteristics of a wide variety of crystal forms. DAC pressurization can be

used to compress an existing crystal, offering the potential for single-crystal-to-single-crystal phase transitions, or to crystallize compounds or mixtures from liquids or from solution. High pressure crystallography has the potential to contribute significantly to the body of knowledge which informs fields such as crystal structure prediction and crystal engineering.[3-5] Crystal structure prediction (CSP) has proven an effective tool in the search for polymorphs of organic compounds in a number of blind tests carried out to determine the reliability of the method.[6-9] CSP calculations provide information on the relationship between density and lattice energy in potential crystal forms. As HP polymorphs of a crystal typically have a higher density, it stands to reason that if a particularly promising polymorph is predicted in the higher density region of the energy surface, a tailored pressurization experiment may be the route to isolating the material experimentally. An example where CSP has correctly predicted a polymorph which was then obtained by a targeted crystallization experiment was the HP crystallization of the drug Dalcetrapib.[5]

One interesting aspect of high pressure crystallization as opposed to ambient or low temperature crystallization routes is the effect it can have on the Z' value of the polymorphs. There are a number of examples where HP crystallization has not only produced a new polymorph of a compound but a higher Z' than seen for the ambient pressure forms. Pyrazine,[10] thiourea[11] and triiodoimidazole all have high pressure polymorphs with Z' higher than the ambient or low pressure forms. Low temperature can also result in high Z' polymorphs; the compounds chloropropamide[12] and tolbutamide have LT polymorphs which have a higher Z' than their ambient forms. Some compounds which undergo multiple transformations on increasing pressure such as urea,[13] toluene[14] and pyrimidine[15] see an initial increase in Z', followed a by a decrease on further crystal transformations. There are also examples of compounds which have a lower Z' in their HP polymorph such as methyl 2-(carbazol-9-yl) benzoate and a derivative of maleic hydrazide.[16, 17] Compression of a single

crystal of the α form of the maleic hydrazine derivative (Z'=4) destabilizes the structure and in order to obtain the high pressure form γ (Z'=1), recrystallization must be carried out *in situ* by compression to 0.4 GPa or above. This γ form can be retrieved from the DAC and is stable at ambient conditions for a long period with no evidence of phase transition or degradation over time.

Our group has recently reported new polymorphs of pyridine-FA cocrystals obtained and studied by high pressure crystallization techniques. [18] Datta and coworker have explored how this system does not obey the ΔpK_a [pK_a (base) – pK_a(acid)] principle used by the pharmaceutical industry to determine if an acid/base combination will produce a salt or a cocrystal on crystallization.[19] Generally if the $\Delta pK_a \geq$ 2-3, a salt will be formed. It was found by the Nangia group that for mixtures of pyridines and carboxylic acids this is not an accurate predictor for salt *vs*. cocrystal formation.[20] Instead a negative ΔpK_a will result in a molecular cocrystal, while above 3.75 a salt will be formed. This leaves an intermediate region $0 < \Delta pK_a > 3.75$ in which either crystal type, or a disordered solid form will be obtained, the prediction of which is made difficult by the nature of the partially polarized O-H···N hydrogen interaction between the pyridine derivative and carboxylic acid. DFT calculations were used by Datta to emphasize how the cooperative enhancement of formic acid acidity plays a large role in determining the nature of the crystallization product, although the results of these calculations suggested that pyridine/formic acid crystals in acid: base ratios lower than 4:1 should be unstable with respect to proton transfer and salt formation. It was concluded from this that at higher stoichiometry, ΔpK_a is not a reliable indicator for proton transfer or potential salt or cocrystal formation.

Here we present the investigation into the highly sterically hindered pyridine analogue 2,6-lutidine (2,6-dimethylpyridine, DMP). DMP is a simple substituted pyridine derivative commonly used as a mild base, as well as a food additive.[21] While DMP is a slightly stronger

Brønsted base than pyridine its steric bulk makes it a weaker hydrogen bond base and hence DMP complexes are expected to give interesting insight into the effect of basicity on HP/LT polymorphism of weak acid-base cocrystals and their propensity to undergo proton transfer. [22, 23] The ΔpK_a of a DMP and formic acid mixtures is 2.95.

Experimental

All mixtures of DMP and FA are liquid at room temperature. All low temperature structures were obtained by *in situ* cryo-crystallization using a 0.3 mm borosilicate glass capillary, loaded with the appropriate mixture, sealed at both ends and affixed to a pin mounted to a goniometer head. Crystals were obtained by a combination of cooling using the cryostream and flash freezing with liquid nitrogen. Once crystals were obtained, the temperature was cycled to obtain a suitable single crystal. An Agilent Xcalibur Gemini diffractometer equipped with Oxford Cryosystems open flow nitrogen cryostat was used for data collection for the 1:2 co-crystal. CrysAlis PRO[24] was used for data processing of the structure. Molecular complexes 1:3 and 1:1 were crystallised on a Bruker SMART CCD 6000 diffractometer using a special mount for bulky attachments that allows better handling of the sample but slightly reduces completeness.[25] The data were processed using SAINT and SADABS software.

Crystals grown at high pressure were obtained by loading the liquid mixtures into a diamond anvil cell with diamond culets of 0.8 mm. Samples occupy a sample chamber created by a steel gasket of 0.25 mm thickness, pre-indented to 0.15 mm with a precision drilled hole of 300 μm. A ruby was included in the sample chamber for pressure determination.[26] The pressure was increased until a polycrystalline phase was obtained, then the pressure was cycled around the melting transition point until a single crystal was obtained of suitable quality and size for diffraction. The sample was pressurized beyond the crystal

growth pressure region in order to minimize melting during data collection. The DAC was mounted directly onto the goniometer of XIPHOS II,[27, 28] a four circle Huber diffractometer with Ag-Kα *IμS*[29] generator located at Newcastle University. High pressure data were handled using the Bruker APEX2[30] software suite which incorporates SAINT[31] and SADABS[32] for integration, cell refinement and scaling. The program ECLIPSE[33] was used to generate dynamic masks to compensate for shading from the body of the DAC. The SHELX[34] program suite was used for structure solution and refinement of all structures within the OLEX2 interface.[35]

Results

Table 1. Summary of crystallographic data.

	HP			LT		
Base: Acid	1:1	1:2	1:3	1:1	1:2	1:3
empirical formula	$C_8H_{11}NO_2$	$C_9H_{13}NO_4$	$C_{10}H_{15}NO_6$	$C_8H_{11}NO_2$	$C_9H_{13}NO_4$	$C_{10}H_{15}NO_6$
T/K	296			230	200	230
P/kbar	0.3	1.5	3.7	ambient		
Crystal system	Orthorhombic		Monoclinic	Orthorhombic	Triclinic	Monoclinic
space group	$Pca2_1$	$P2_12_12_1$	Pn	$Pca2_1$	$P\bar{1}$	$P2_1/c$
a/Å	15.554(2)	3.969(2)	4.0173(7)	15.723(4)	7.914(2)	3.974(1)
b/Å	7.030(1)	24.22(2)	10.155(2)	7.137(1)	7.975(2)	14.993(5)
c/Å	7.3617(6)	10.116(9)	14.764(5)	7.497(1)	9.861(2)	20.717(7)
α	90	90	90	90	69.68(2)	90
β	90	90	92.64(2)	90	81.57(2)	92.19(2)
γ	90	90	90	90	64.75(2)	90
Z	4	4	2	4	2	4
Z'	1	1	1	1	1	1
V/Å^3	805.0(1)	972(1)	601.7(3)	841.3(3)	527.8(2)	1233.4(7)
D_c/g cm^{-3}	1.264	1.368	1.354	1.209	1.253	1.321
Unique reflns.	2965	2223	1747	2965	4346	11137
completeness/ %	83	62	52	83	100	78

R_1	0.0497	0.0815	0.0596	0.0497	0.0691	0.0784
wR_2	0.12676	0.2913	0.1694	0.1267	0.1703	0.2646
GOF	1.035	1.113	1.076	1.035	1.0140	0.996

Table 2. N-H···O bond distances and angles for all structures.

	Donor	Hydrogen	Acceptor	DH/Å	HA/Å	DA/Å	DHA/°
1:1 HP	O9	H9	N1	1.02(10)	1.6(1)	2.589(8)	170(9)
1:1 LT	O9	H9	N1	0.83(2)	1.8(1)	2.616(3)	155(3)
1:2 HP	N1	H1	O9	1.0(2)	1.80(2)	2.64(3)	165(1)
1:2 LT	N1	H1	O9	1.06(4)	1.62(4)	2.673(3)	176(4)
1:3 HP	N1	H1	O9	0.86(1)	1.96(1)	2.80(2)	163(2)
1:3 LT	N1	H1	O9	0.99(3)	1.80(3)	2.771(3)	165(3)

1:1 DMP-FA

Both slow cooling and pressurizing DMP and FA in a 1:1 ratio affords a stoichiometric molecular cocrystal. The same polymorph is obtained from both the HP and LT crystallization methods, with one molecule of each compound in the asymmetric unit. The dominant interaction is a hydrogen bond between the O-H group of FA and the nitrogen atom of the pyridyl ring of DMP, at a DA distance of 2.589(8) Å and 2.616(3) in the HP and LT crystals, respectively (Table 2). The DMP pyridyl rings interact via π-π stacking at a plane-centroid distance of 3.6830(3) Å and offset shift of 1.385(9) Å measured from the LT dataset, shown in Figure 1 where the distance d_1 is the place-centroid distance, d_2 is the centroid-centroid distance and s is the shift.

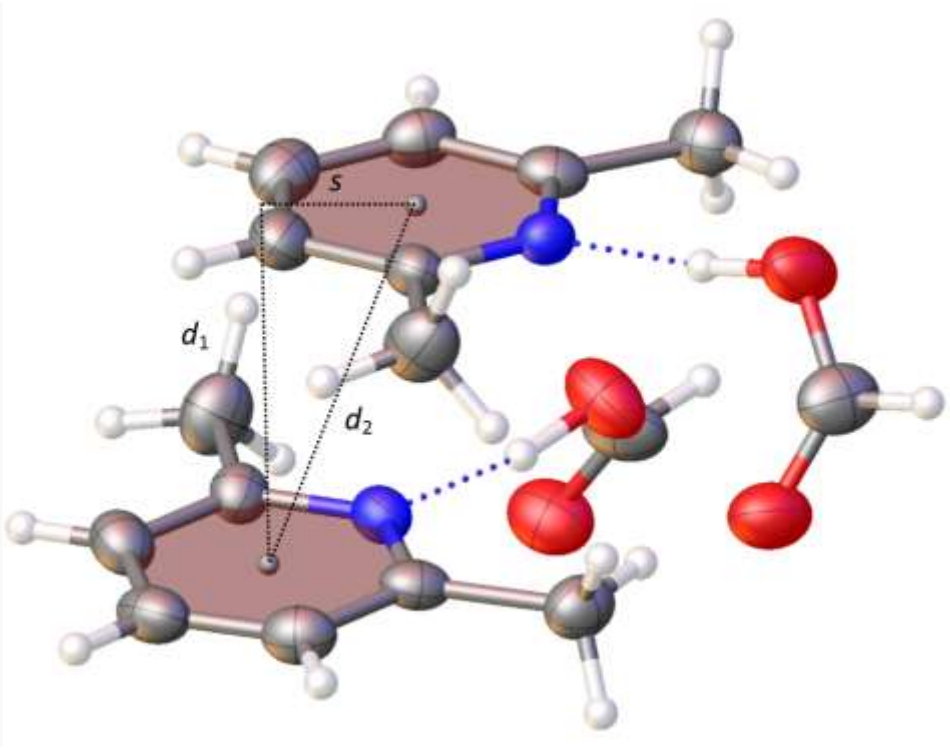

Figure 1. π-π stacking interactions of DMP- FA crystallized with high pressure.

A comparison of the unit cell volume shows a compression of 4.3% in the HP structure relative to the LT form. The temperature difference of 66 K is a contributor to the change in cell volume, so this unit cell volume difference does not accurately represent the extent of the compressibility of the structure. Data for the HP crystal were collected at 0.3 kbar (Table 1).

1:2 DMP-FA

A 1:2 mixture of DMP and FA crystallizes *via* both HP and LT crystallization methods. At this higher concentration of acid, HP/LT polymorphism is seen. While the HP structure crystallizes in orthorhombic space group $P2_12_12_1$, the symmetry is lower in the LT form which is triclinic space group $P\bar{1}$. In the HP structure, the molecules are more closely packed, with a unit cell packing efficiency of 66% compared with 63% for the LT form.

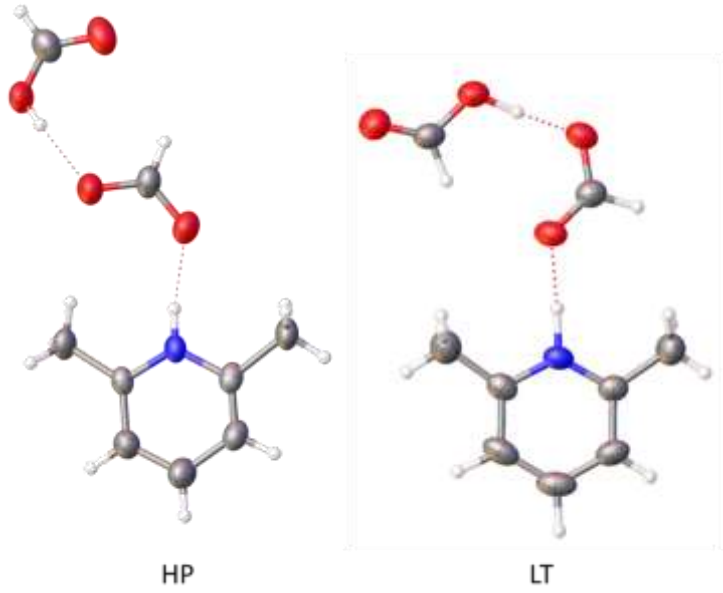

Figure 2. 2,6-dimethylpyridinium formate formic acid cocrystal asymmetric units from HP and LT crystallization.

As with the pyridine analogue, an increased acid/base ratio strengthens the AH···B hydrogen bond interaction resulting in proton transfer between the pyridyl ring and FA, giving rise to a 2,6-dimethylpyridinium formate formic acid salt cocrystal from both crystallization routes (Figure 2).[18, 19, 36] With a ΔpK_a of 2.95, the DMP-FA mixtures fall in the intermediate ΔpK_a region of salt/cocrystal formation for pyridines and carboxylic acids. This 1:2 salt formation is influenced by the cooperative nature of the FA molecules enhancing acidity and therefore proton transfer at stoichiometries higher than 1:1, the same effect which is seen in the pyridine-FA mixtures.

Each polymorph of 1:2 DMP-FA contains one DMP-H^+ ion, a formate ion and a molecule of formic acid in a planar arrangement, with a charge assisted hydrogen bond between the 2,6-dimethylpyridinium and formate ions. The relative orientations of the formate and formic acid groups to DMP-H^+ differ between the HP and LT forms (Figure 2) resulting in a considerable change in symmetry and unit cell parameters (Table 1).

The hydrogen bond distances of the NH···O hydrogen interaction between DMP-H^+ and formate are 2.64(3) and 2.673(3) Å for HP and LT, respectively (

Table 3). The charge assisted hydrogen bond in the higher ratio cocrystal is a critical factor in determining molecular packing motif but the ion-ion interaction between DMP-H^+ and formate is also a consideration. The OH···O bond distance in the 1:2 polymorphs is 2.516(4) for the LT form and 2.48(3) for HP.

Table 3. Hydrogen bonding parameters of 1:2 DMP-FA HP

	D	H	A	DH/ Å	HA/ Å	DA/ Å	DHA/ °
HP	N1	H1	O9	1.0(2)	1.80(2)	2.64(3)	165(1)
	O12	H12	O11	0.82(2)	1.78(2)	2.48(3)	142(1)
LT	N1	H1	O9	1.06(4)	1.62(4)	2.673(3)	176(4)
	O12	H12	O11	1.03(5)	1.49(5)	2.516(4)	177(4)

If we consider the DMP-formate-formic acid arrangement in each structure to be the 'synthon' for that form, the synthons have significantly different packing arrangements in each crystal structure. In the LT polymorph, the synthons pack *via* weak CHO interactions and off-set π-π stacking between pyridyl rings into discrete layers in the (440) plane. The HP polymorph has a more complex packing arrangement, as shown in Figure 3.

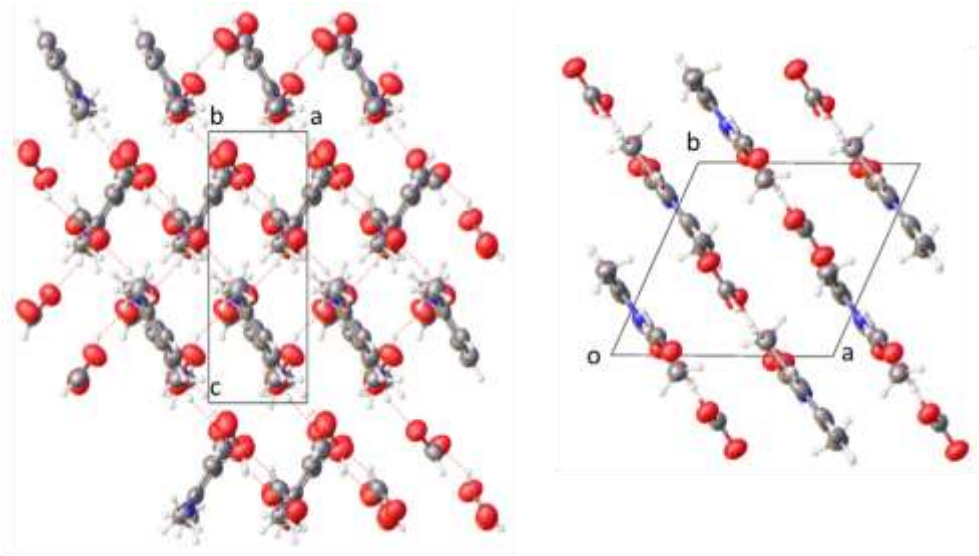

Figure 3. Packing arrangements of 1:2 DMP-FA from HP (left) and LT (right) crystallisation.

Offset π-π stacking is present in both HP and LT forms, although the interaction is closer in the LT form with a shift of 1.829(7) Å and distance 3.869(3) Å compared with shift of 2.13(4) Å and distance 3.969(2) Å in the HP polymorph, suggesting it is a more dominant interaction in the LT configuration.

1:3 DMP-FA

Mixtures of DMP and FA in ratios 1:3 and higher, crystallize in a 1:3 structure. This concentration also exhibits HP/LT polymorphism, although it is more subtle than that seen for the 1:2 cocrystal. Figure 4 shows the asymmetric units of the 1:3 cocrystals from DAC crystallization and capillary crystallization. Both have undergone proton transfer during crystallization and contain one 2,6-dimethylpyridinium ion, a formate ion and two molecules of formic acid, in a hydrogen bonded synthon. While the unit cell parameters for the two forms are very similar to one another (Table 1) the details of the packing arrangement reveals that the crystals are two distinct polymorphs. The primary difference between the asymmetric units is the orientation of the FA groups relative to the primary DMP-H^+-formate hydrogen bond interaction.

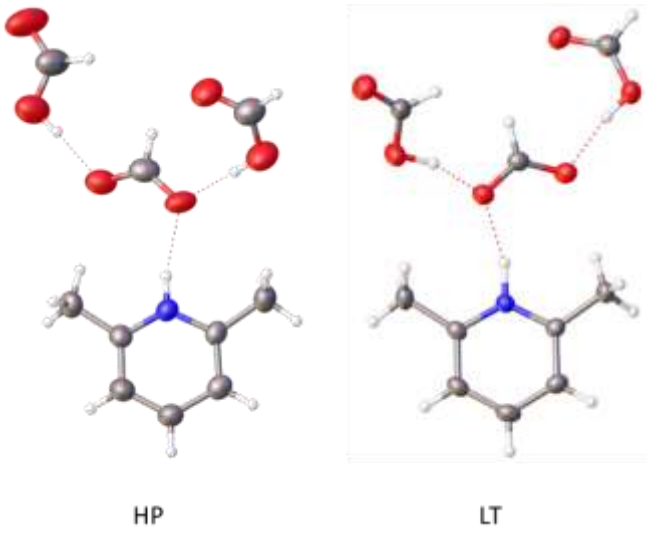

Figure 4. Asymmetric unit of 1:3 DMP-FA cocrystals.

An overlay of the two structures (Figure 5) shows that while the DMP-H^+ – formate interaction is largely the same, the two FA molecules are 'flipped' relative to each other, as if rotated around the C-O bonds O12-C13 and O15-C16.

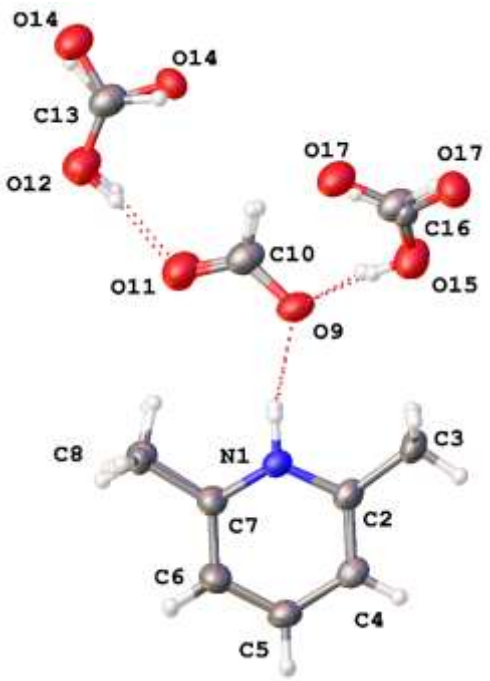

Figure 5. Overlay of HP and LT structures of 1:3 2,6-dimethylpyridinium formate bis(formic acid).

While DMP has a 1:3 ratio with FA, pyridine forms a 1:4 structure and no evidence of a 1:3 form has been observed.[18] Due to the methyl groups on DMP, FA molecules cannot pack closely around the pyridyl ring as seen for pyridine-FA (Figure 6). A 1:4 mixture of DMP and FA acid was found to crystallize in the 1:3 form. The steric hindrance also causes the nature of the charge assisted hydrogen bond to differ between the cocrystal analogues; the pyridinium ion in 1:4 pyridine-FA displays a bifurcated hydrogen bonding pattern to two FA molecules, whereas all of the DMP cocrystals with FA retain the highly directional NHO bond regardless of proton transfer or lack thereof.

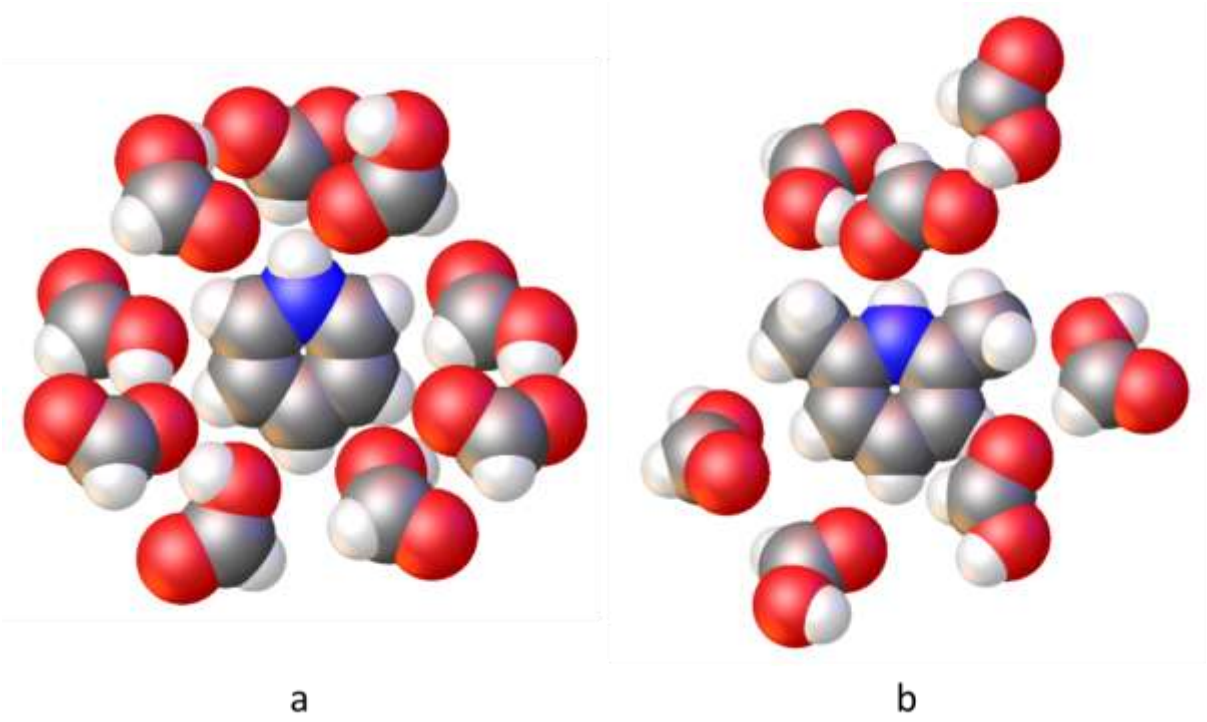

Figure 6. Space-filling packing diagrams showing the environment of the pyridyl ring in a) HP 1:4 pyridine-FA and b) HP 1:3 DMP-FA.

Table 4. Hydrogen bond parameters of HP and LT polymorphs of 1:3 DMP-FA

	D	H	A	DH	HA	DA	DHA
HP	N1	H1	O9	0.86(1)	1.96(1)	2.80(2)	163(2)
	O15	H15	O9	0.82(2)	1.79(1)	2.60(2)	172(1)
	O12	H12	O11	0.82(2)	1.84(1)	2.56(2)	150(1)
LT	N1	H1	O9	0.99(3)	1.80(3)	2.771(3)	165(3)
	O15	H15	O9	1.02(6)	1.58(6)	2.566(4)	162(5)
	O12	H12	O11	0.83(3)	1.75(6)	2.562(3)	167(1)

The donor···acceptor distances are remarkably similar between the two structures, emphasizing the subtlety of the polymorphism in this system (Table 4). The largest difference is seen in the DHA bonding angles, particularly between the formate ion and one FA molecule; the angle O12-H12-O11 has a difference of 17° between polymorphs.

Discussion

All of the DMP-FA cocrystals display relatively strong, directional hydrogen bonds between the DMP and FA components (Table 2), including the higher ratio structures. The hydrogen bond type is evident in the DA bond distances; shortest for HP 1:1 DMP-FA at 2.589(8) Å a neutral interaction, but longer distances of 2.64(3) Å and 2.798(17) Å for the HP 1:2 and 1:3 cocrystals, respectively.

In the 1:4 pyridine-FA cocrystal[17] the ion-ion interaction of pyridinium and formate ions takes precedence over strong directional hydrogen bonding in the crystal packing and there are two weaker hydrogen bonding interactions between the pyridyl nitrogen and formic acid molecules as opposed to a single, more directional bond, which is present in all DMP-FA cocrystals reported here. The methyl groups of DMP have the combined effect of sterically hindering the pyridyl nitrogen atom and increasing its Brønsted basicity relative to pyridine.[21] The methyl substitution does not appear to have an effect on proton transfer despite DMP being a slightly stronger base than pyridine, with a pKa$_H$ of 6.8 compared with 5.2, where pKa$_H$ is the pKa of the conjugate acid.[12] In both instances, proton transfer occurs for an acid/base ratio of 2 or higher. The difference in the Brønsted basicity between the two heteroaromatic rings is reflected in the hydrogen bond lengths in the higher ratio crystal structures, for both HP and LT forms of DMP-FA and pyridine-FA cocrystals. The HA and DA hydrogen bonding distances are consistently shorter for the DMP cocrystals, due the higher basicity of 2,6-dimethylpyridine. In the HP form of 1:3 DMP-FA the N-H···O charge assisted hydrogen bond has a DA distance of 2.80(2) Å, while the equivalent bond in 1:4 pyridine-FA has a distance of 2.853(10) Å. There is a larger difference for the equivalent LT forms with 1:3 DMP-FA having an N-H···O distance of 2.771(3) Å compared with 2.870(3) for the pyridine analogue. The bifurcated nature of the hydrogen bonding in the pyridine-FA cocrystal contributes to the longer D…A distances. Such bifurcation is not possible with

DMP due to the steric hindrance of the methyl groups adjacent to the pyridyl nitrogen. The relative basicity has a significant effect on the bonding distances and this is seen also for the 1:1 cocrystals of both heteroaromatic rings, where in each case there is a strong, directional hydrogen bond between neutral molecules. The D-A distance for this bond in the 1:1 DMP-FA structure is 2.589(8) Å and 2.634(12) for the pyridine-FA.

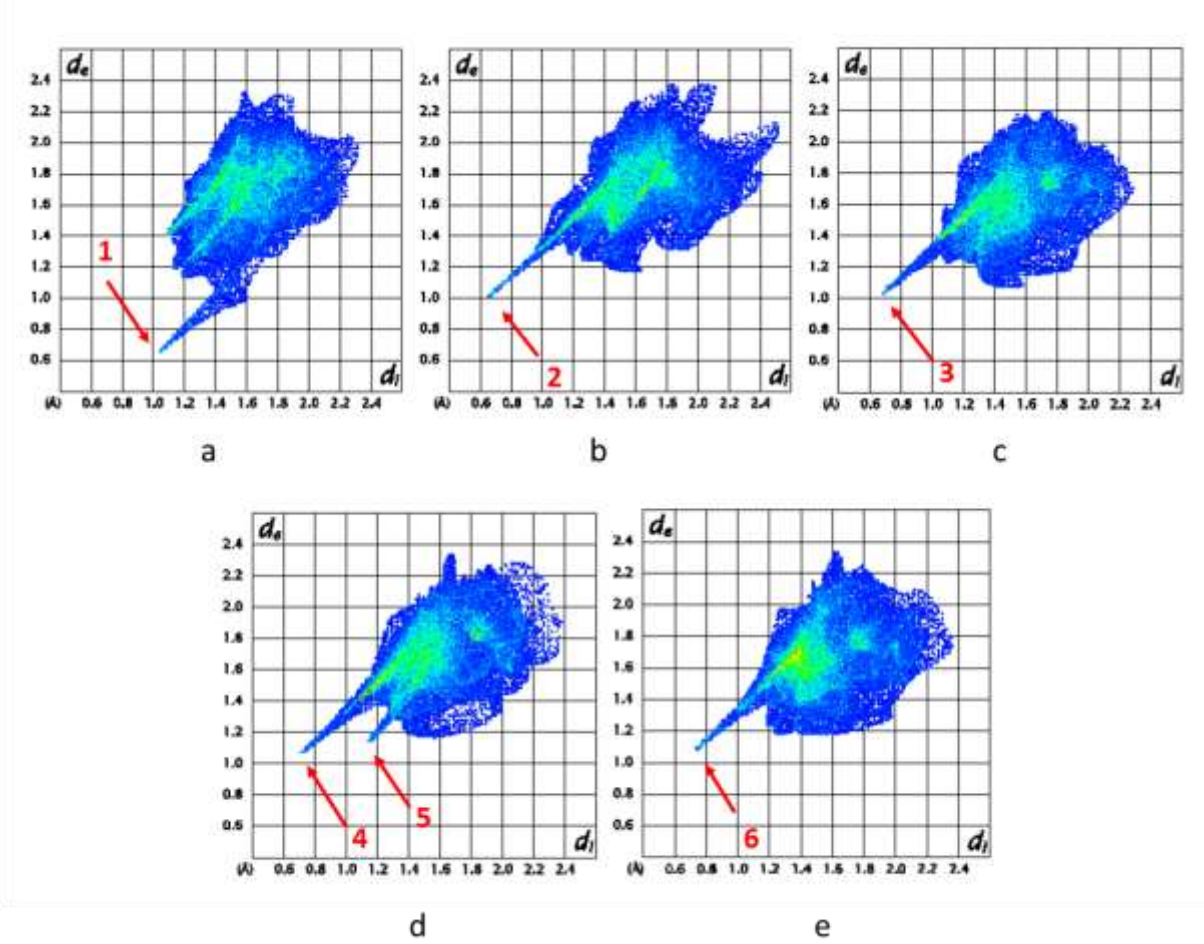

Figure 7. Hirshfeld surface fingerprint plots of DMP in DMP-FA co-crystals; a) 1:1 LT, b) 1:2 LT, c) 1:2 HP, d) 1:3 LT and e) 1:3 HP, showing features from N-H interactions (1) O-H interactions (2-4, 6) and H-H interactions (5).

Fingerprint plots generated from Hirshfeld surfaces using the visualization tool Crystal Explorer offer a useful way of representing the intermolecular interactions within a crystal and differences in bonding between polymorphs and comparable cocrystals. [37, 38, 39] The

program generates a Hirshfeld surface around a selected atom or group and plots the proximity of other atoms or groups to this surface using values d_e, the distance between the Hirshfeld surface and the nearest external contact and d_i, the distance between the surface and the nearest internal contact. This plot is known as a fingerprint plot.

Figure 7 shows the fingerprint plots for the Hirshfeld surface of DMP/ DMP-H^+ for each polymorph of DMP-FA. The plots show the following differences in the nature of intermolecular contacts within the structure. In Figure 7a, the feature labelled 1 is due to the N···H interaction between the nitrogen of DMP and the acidic proton of FA, a neutral hydrogen bonding interaction. As proton transfer has occurred in the other four structures this peak is no longer seen, but a new feature at higher d_e appears labelled 2,3,4 and 6, as a result of the N-H···O charge assisted hydrogen bond interaction. When the regions of the fingerprint plot relating to individual atom type are isolated, it can be determined that the contribution of N···H interactions in plots *b-e* is less than 1%, while for *a*, it is 6.6%.

For all of the structures, the majority of the surface interaction is due to H···H interactions, which make up the bulk of the blue area and the features in the top right of each plot. However in plot Figure 7d (1:3 LT) the peak labelled 5 is also due to H···H interactions, in closer contact than seen in any other DMP-FA structure including the HP 1:3 polymorph. This is due to the atom H8C on one of the methyl groups of DMP; crystal packing brings this hydrogen atom into close contact with equivalent H8C atoms on neighboring DMP-H^+ in adjacent layers. This is an unusual feature not seen for the other high pressure cocrystals of DMP and pyridine, which instead show changes to the more diffuse region of the fingerprint plot which represents the bulk of H···H contacts, rather than an enforced short contact In the HP plots, this diffuse H···H region is more compact than in the LT versions as molecules are encouraged into closer contact by the application of pressure.

Conclusions

Mixtures of 2,6-dimethylpyridine and formic acid offer a good example of high pressure/ low temperature polymorphism analogous to that seen for the similar pyridine formic acid systems.

A 1:1 mixture of DMP and FA affords a neutral cocrystal with the same polymorph obtained from both HP and LT crystallization methods. Higher acid concentration forms 1:2 and 1:3 afford salt cocrystals with components in the expected acid/base ratio although proton transfer between the acid and base has occurred resulting in charge-assisted hydrogen bonding interactions. This is potentially a contributing factor in the HP/LT polymorphism of the system, given the lack of polymorphism in the neutral molecular cocrystal of 1:1 DMP-FA.

The use of Hirshfeld surface fingerprint plots has clearly indicated structural differences between polymorphs that are otherwise not obvious from inspection of the unit cell and packing of a structure as is the case for the 1:3 polymorphs of DMP-FA, which exhibit subtle differences between polymorphs.

Notes

Corresponding author: *michael.probert@ncl.ac.uk

Acknowledgements

We thank Bruker UK Ltd. for funding.

Supporting information

Supporting information is available: CCDC codes 1517433-1517438 contain crystallographic information for this paper.

References

(1) Lee, R.; Howard, J. A. K.; Probert, M. R.; Steed, J. W.; *Chem. Soc. Rev.* **2014**, *43*, 4300-4311.

(2) Boldyreva, E.; *Acta Crystallographica Section A* **2008**, *64*, 218-231.

(3) Ridout, J.; Price, L. S.; Howard, J. A. K.; Probert, M. R.; *Cryst. Growth Des.* **2014**, *14*, 3384-3391.

(4) Oswald, I. D. H.; Allan, D. R.; Day, G. M.; Motherwell, W. D. S.; Parsons, S.; *Cryst. Growth Des.* **2005**, *5*, 1055-1071.

(5) Neumann, M. A.; van de Streek, J.; Fabbiani, F. P. A.; Hidber, P.; Grassmann, O.; *Nat Commun* **2015**, *6*,

(6) Kazantsev, A. V.; Karamertzanis, P. G.; Adjiman, C. S.; Pantelides, C. C.; Price, S. L.; Galek, P. T. A.; Day, G. M.; Cruz-Cabeza, A. J.; *Int. J. Pharm.* **2011**, *418*, 168-178.

(7) Day, G. M.; Motherwell, W. D. S.; Ammon, H. L.; Boerrigter, S. X. M.; Della Valle, R. G.; Venuti, E.; Dzyabchenko, A.; Dunitz, J. D.; Schweizer, B.; van Eijck, B. P.; Erk, P.; Facelli, J. C.; Bazterra, V. E.; Ferraro, M. B.; Hofmann, D. W. M.; Leusen, F. J. J.; Liang, C.; Pantelides, C. C.; Karamertzanis, P. G.; Price, S. L.; Lewis, T. C.; Nowell, H.; Torrisi, A.; Scheraga, H. A.; Arnautova, Y. A.; Schmidt, M. U.; Verwer, P.; *Acta Crystallogr., Sect. B: Struct. Sci.* **2005**, *61*, 511-527.

(8) Lommerse, J. P. M.; Motherwell, W. D. S.; Ammon, H. L.; Dunitz, J. D.; Gavezzotti, A.; Hofmann, D. W. M.; Leusen, F. J. J.; Mooij, W. T. M.; Price, S. L.; Schweizer, B.; Schmidt, M. U.; van Eijck, B. P.; Verwer, P.; Williams, D. E.; *Acta Crystallogr., Sect. B: Struct. Sci.* **2000**, *56*, 697-714.

(9) Motherwell, W. D. S.; Ammon, H. L.; Dunitz, J. D.; Dzyabchenko, A.; Erk, P.; Gavezzotti, A.; Hofmann, D. W. M.; Leusen, F. J. J.; Lommerse, J. P. M.; Mooij, W. T. M.; Price, S. L.; Scheraga, H.; Schweizer, B.; Schmidt, M. U.; van Eijck, B. P.; Verwer, P.; Williams, D. E.; *Acta Crystallogr., Sect. B: Struct. Sci.* **2002**, *58*, 647-661.

(10) Patyk, E.; Podsiadło, M.; Katrusiak, A.; *Cryst. Growth Des.* **2015**, *15*, 5670-5674.

(11) Tomkowiak, H.; Olejniczak, A.; Katrusiak, A.; *Cryst. Growth Des.* **2013**, *13*, 121-125.

(12) Seryotkin, Y. V.; Drebushchak, T. N.; Boldyreva, E. V.; *Acta Crystallogr., Sect. B: Struct. Sci.* **2013**, *69*, 77-85.

(13) Olejniczak, A.; Ostrowska, K.; Katrusiak, A.; *J. Phys. Chem. C* **2009**, *113*, 15761-15767.

(14) Marciniak, J.; Bąkowicz, J.; Dobrowolski, M. A.; Dziubek, K. F.; Kaźmierczak, M.; Paliwoda, D.; Rajewski, K. W.; Sobczak, S.; Stachowicz, M.; Katrusiak, A.; *Cryst. Growth Des.* **2016**, *16*, 1435-1441.

(15) Patyk, E.; Podsiadło, M.; Katrusiak, A.; *Cryst. Growth Des.* **2015**, *15*, 4039-4044.

(16) Johnstone, R. D. L.; Ieva, M.; Lennie, A. R.; McNab, H.; Pidcock, E.; Warren, J. E.; Parsons, S.; *CrystEngComm* **2010**, *12*, 2520-2523.

(17) Roszak, K.; Katrusiak, A.; Katrusiak, A.; *Cryst. Growth Des.* **2016**, *16*, 3947-3953.

(18) Lee, R.; Firbank, A. J.; Probert, M. R.; Steed, J. W.; *Cryst. Growth Des.* **2016**, *16*, 4005-4011.

(19) Pratik, S. M.; Datta, A.; *The Journal of Physical Chemistry B* **2016**, *120*, 7606-7613.

(20) Bhogala, B. R.; Basavoju, S.; Nangia, A.; *CrystEngComm* **2005**, *7*, 551-562.

(21) PubChem Compound Database. https://pubchem.ncbi.nlm.nih.gov/compound/7937 (Oct 20, 2016),

(22) Grandberg, I. I.; Faizova, G. K.; Kost, A. N.; *Chem. Heterocycl. Compd. (N. Y., NY, U. S.)* **1967**, *2*, 421-425.

(23) Laurence, C.; Berthelot, M.; *Perspect. Drug Discovery Des.* **2000**, *18*, 39-60.

(24) Agilent *CrysAlis PRO*, Agilent Tecnologies Ltd: Yarnton, Oxfordshire, UK, 2014.

(25) Yufit, D. S.; Howard, J. A. K. H; *J.Appl.Crystallogr.* **2005**, *38*, 583-586

(26) Forman, R. A.; Piermarini, G. J.; Barnett, J. D.; Block, S.; *Science* **1972**, *176*, 2.

(27) Probert, M. R.; Robertson, C. M.; Coome, J. A.; Howard, J. A. K.; Michell, B. C.; Goeta, A. E.; *J. Appl. Crystallogr.* **2010**, *43*, 1415-1418.

(28) Probert, M. R.; Coome, J. A.; Goeta, A. E.; Howard, J. A. K.; *Acta Crystallographica Section A* **2011**, *67*, C528.

(29) Schulz, T.; Meindl, K.; Leusser, D.; Stern, D.; Graf, J.; Michaelsen, C.; Ruf, M.; Sheldrick, G. M.; Stalke, D.; *J. Appl. Crystallogr.* **2009**, *42*, 885-891.

(30) *APEX2*, 1.08; Bruker AXS Inc.: Madison, WI, 2004.

(31) *SAINT*, Bruker AXS Inc.: Madison, WI, 2007.

(32) *SADABS*, Bruker AXS Inc.: Madison, WI, 2001.

(33) Parsons, S., ECLIPSE In ed.; Edinburgh, UK, 2010.

(34) Sheldrick, G.; *Acta Crystallographica Section C* **2015**, *71*, 3-8.

(35) Dolomanov, O. V.; Bourhis, L. J.; Gildea, R. J.; Howard, J. A. K.; Puschmann, H.; *J. Appl. Crystallogr.* **2009**, *42*, 339-341.

(36) Balevicius, V.; Bariseviciute, R.; Aidas, K.; Svoboda, I.; Ehrenberg, H.; Fuess, H.; *PCCP* **2007**, *9*, 3181-3189.

(37) Spackman, M. A.; Jayatilaka, D.; *CrystEngComm* **2009**, *11*, 19-32.

(38) Spackman, M. A.; McKinnon, J. J.; *CrystEngComm* **2002**, *4*, 378-392.

(39) *CrystalExplorer (Version 3.1),* S.K. Wolff, D.J. Grimwood, J.J. McKinnon, M.J. Turner, D. Jayatilaka, M.A. Spackman, University of Western Australia, 2012.

For use in Table of Contents Only:

High Pressure/ Low Temperature Polymorphism in 2,6-Dimethylpyridine Formic Acid Cocrystals.

Rachael Lee, Dmitry S. Yufit, Michael R. Probert, Jonathan W. Steed

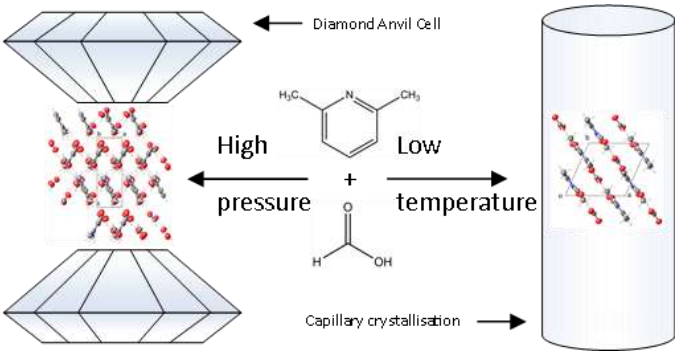

Synopsis:

Concentration dependent high pressure/low temperature polymorphism is explored in the acid-base liquid system 2,6-dimehtylpyridine and formic acid, utilizing *in situ* non-ambient crystallisation conditions of the diamond anvil cell and capillary crystallisation.